



Using coupled fish behavior–hydrodynamic model to investigate spawning migration of Japanese anchovy, *Engraulis japonicus*, from the East China Sea to Taiwan

CHEN-YI TU,¹ YU-HENG TSENG,²
TAI-SHENG CHIU,³ MAO-LIN SHEN²
AND CHIH-HAO HSIEH^{1*}

¹Institute of Oceanography, National Taiwan University, 1 Roosevelt Rd., Sec. 4, Taipei 10617, Taiwan

²Department of Atmospheric Sciences, National Taiwan University, 1 Roosevelt Rd., Sec. 4, Taipei 10617, Taiwan

³Institute of Zoology, National Taiwan University, 1 Roosevelt Rd., Sec. 4, Taipei 10617, Taiwan

ABSTRACT

Adult Japanese anchovies (*Engraulis japonicus*) migrate from the East China Sea to the coastal region of Taiwan to spawn around late winter and early spring and, later, their larvae constitute important fisheries in Taiwan. However, their migration route and its mechanism remain unclear. To investigate their spawning migration, we used a coupled fish behavior–hydrodynamic modeling approach. The physical field is simulated by the Pacific Ocean adaptation of the Taiwan Multi-scale Community Ocean Model (TIM-COM) and the fish migration by Lagrangian tracer tracking with the aid of approximation of fish swimming behavior. We investigated three fish behavioral scenarios: (i) passive tracking of the current, (ii) swimming along with the current, and (iii) swimming along with the current and then changing to swimming toward the optimal spawning temperature. The comparison with and without Changjiang discharge is used to investigate the impacts of discharge reduction due to the Three Gorges Dam. Our results suggest that spawning migration of Japanese anchovy from the East China Sea to Taiwan may be aided by the China Coastal Current and that adult anchovies cannot reach the spawning site by passive advection alone. Thus, the swimming behavior of anchovies is crucial during the spawning migration, as it provides extra

velocity and the orientation to the favorable spawning grounds. In addition, the adult anchovy is unlikely to reach the coastal area of Taiwan without Changjiang discharge. Our findings indicate that a coupled fish behavior–hydrodynamic model can help understand the influences of physical environment on the migration of Japanese anchovies.

Key words: Changjiang discharge, China Coastal Current, fish swimming behavior model, Japanese anchovy, physical–biological coupling, recruitment processes, spawning migration

INTRODUCTION

The anchovy fishery (targeting the larvae) is one of the most important commercial fisheries in the coastal waters of Taiwan of the western North Pacific. In northern Taiwan, the anchovy catches are mainly composed of Japanese anchovy (*Engraulis japonicus*). Although the larval anchovy fishery is substantial, the adult anchovies do not form a significant fishery around Taiwan, as no adult anchovy population is found around Taiwan after their spawning season. By contrast, the adult anchovies are important targets in mainland China in the East China Sea (ECS; Yu *et al.*, 2005). Fishery acoustic surveys on adult Japanese anchovies (Iversen *et al.*, 1993) show that the ECS is likely a natural feeding ground. According to genetic analyses, several groups of adult Japanese anchovies exist in the ECS (Yu *et al.*, 2002, 2005). Larval surveys combined with fisheries records indicate that the coastal region of Taiwan is an important spawning ground of Japanese anchovy (Chen and Chiu, 2003). Combining this evidence, it is believed that at least one population of adult anchovies migrates to the coastal areas of Taiwan to spawn and then leaves after spawning (Chen and Chiu, 2003; Lee *et al.*, 2009). However, the exact migration route and possible processes determining their spawning migration remain largely unknown (Chen *et al.*, 2010).

Success in the spawning migration potentially affects larval recruitment (Cushing, 1975). In addition,

*Correspondence. e-mail: chsieh@ntu.edu.tw

Received 1 April 2011

Revised version accepted 9 December 2011

the Member–Vagrancy hypothesis (Sinclair, 1988) may apply: successful recruitment can only happen if the adult fishes spawn at certain places in which the physical environment favors the retention of eggs and larvae. In the case of Japanese anchovy, the year-round cold eddy near the coastal waters of northeastern Taiwan (Tang *et al.*, 2000) makes a favorable spawning ground (Chen and Chiu, 2003). Thus, the spawning migration of Japanese anchovies from the ECS to Taiwan is biologically reasonable. The fishing season of larval anchovies, which starts from spring, peaks in March and gradually diminishes in summer (Fig. 1b), suggests that the spawning migration may start in winter. Considering the seasonal variation of circulation in the ECS and the coastal area of Taiwan, the only southward current in winter and early spring is the China Coastal Current (CCC). It is therefore suggested that Japanese anchovies may take advantage of the CCC to move southward to the spawning

grounds (Chen *et al.*, 2010) (Fig. 2). However, this hypothesis has never been tested. Obviously, it is difficult to operate a large-scale field survey to locate the spawning stock on the move.

To investigate the spawning migration of Japanese anchovies, we used a coupled biological–physical model. With the advances in computation and hydrodynamic modeling, the use of Lagrangian particle tracking simulation to study the dispersal and migration of marine organisms has become an important tool in recent years (e.g., Capella *et al.*, 1992; Rose, 1993; Cowen *et al.*, 2006). The advantage of this approach lies in the convenience of investigating different environmental scenarios. Also, the behavior of particles can be explicitly defined to investigate the role of behavior in dispersal/migrating processes. Previous research using Lagrangian particle tracking simulation has demonstrated the usefulness of the modeling approach in providing possible explanations for observed transport and distribution patterns of marine organisms (Miller, 2007). Such a modeling approach combined with behavioral approximation has also been used for simulating the spawning migration of various fish species, e.g., cod and capelin by Huse *et al.* (2004) and Japanese sardine by Okunishi *et al.* (2009).

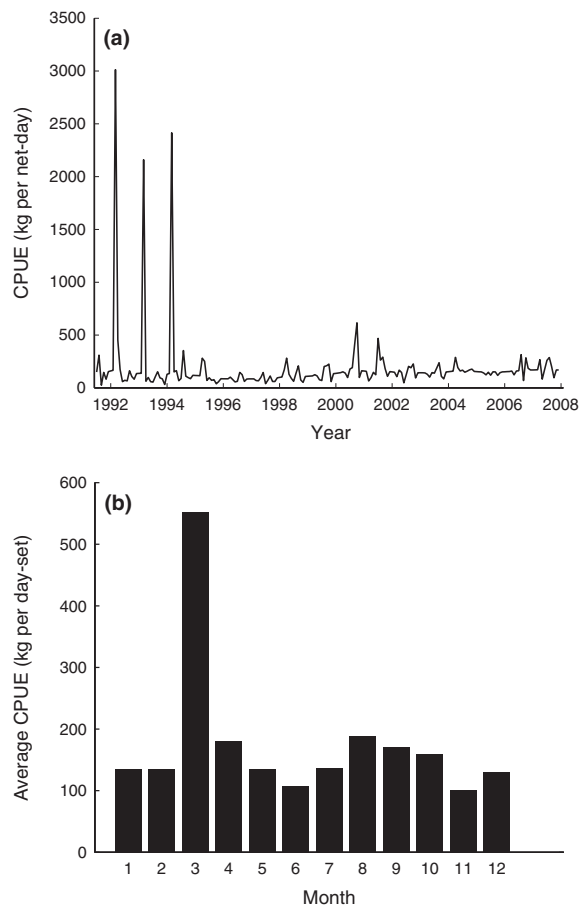
In this study, we hypothesize that the spawning migration of Japanese anchovies is aided by the CCC in the ECS. The spawning migration is simulated by a physical–biological coupled model. The physical component consists of an ocean circulation model. The Changjiang discharge is also included for investigating the potential influence of reduction in discharge caused by the Three Gorges Dam (TGD). The biological component is the Lagrangian particle tracking program, simulating fish migration with a primary approximation of fish swimming behavior. The model simulations are used to clarify the possible migration routes. The results from this research may improve our understandings in the recruitment processes of Japanese anchovies and provide useful information for fishery managements.

MATERIALS AND METHODS

Fisheries data

The larval anchovy fishery is mainly operated in Yilan Bay, northeastern Taiwan (see Fig. 2). Monthly catch per unit effort (CPUE) was used as an estimate of the abundance of larval anchovy stocks from January 1992 to May 2008 (Fig. 1a). The catch and effort data were obtained from logbooks of each trawler pair monthly, with the fishing effort standardized to ‘kg per net-day’

Figure 1. Monthly catch per unit effort (CPUE) (a) and seasonality of the CPUE data (b) of Japanese anchovy larvae.



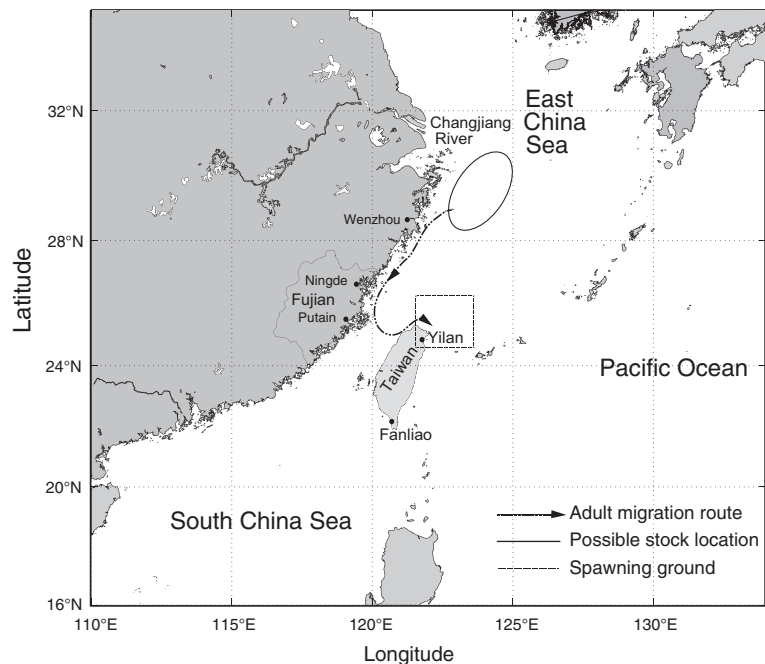


Figure 2. Potential migration route of Japanese anchovy. The spawning group may move southward with the aid of China Coastal Current.

(Chiu *et al.*, 1997). Missing CPUE data were estimated by the state–space reconstruction method (Ljung, 1999; Hsieh *et al.*, 2009). The seasonal average of CPUE indicates that the fishing season of larval anchovies starts in spring, peaks in March, and gradually diminishes in summer (Fig. 1b).

Physical model

The physical model was simulated by the Dual-grid Pacific Ocean Model (DUPOM), which is based on one of the standard configurations of the Taiwan Multi-scale Community Ocean Model (TIMCOM) using two domains covering the entire North Pacific Ocean (Tseng *et al.*, 2010; Shen *et al.*, 2011; Tseng *et al.*, in press). The model is driven by the climatological wind/surface condition and based on a mix of collocated Arakawa-A and staggered Arakawa-C grids. The model domain covers the entire North Pacific Ocean ranging from 30°S to 60°N and from 100°E to 80°W. A 1/8 resolution is used in the domain west of 150°E to resolve the detailed regional circulations. The two domains are fully two-way-coupled at each coarser time step (time steps are finer for the domain with a finer grid spacing) with an overlapping single coarse grid (i.e., 2×2 in fine grid cells). The meander and eddy exchanges are seamless at the interface without intergrid sponge layers or special treatments. Further details about the multiple-grid approach can be found in Dietrich *et al.* (2008). Model bathymetry is interpolated from unfiltered ETOPO2 depth data supplemented with the 1-min depth archive in the

Asian seas provided by the Ocean Data Bank of National Science Council, Taiwan. The vertical resolution is linear-exponentially stretched by 26 layers, with a 6-m-thick top layer. Both grids share the same vertical resolution. Within each grid, longitudinal resolution is uniform and latitudinal resolution is generated such that varying latitude and longitude grid increments are equal everywhere (Mercator grid). The wind forcing of DUPOM is the interpolated monthly Hellerman wind stresses (Hellerman and Rosenstein, 1983). Levitus 94 climatology (Levitus and Boyer, 1994) is used to initialize the model and determine its surface sources of heat and fresh water using the non-damping approach described in Dietrich *et al.* (2004). Our objective is to explore different environmental and behavioral scenarios. Therefore, to avoid complexity arising from interannual variation in the physical environment, we did not use realistic wind forcing.

To investigate the potential effects of TGD located upstream of Changjiang, we simulated our physical model with and without Changjiang discharge (Table 1). We used monthly Changjiang discharge data compiled by the Global Runoff Data Centre of the Federal Institute of Hydrology in Germany (GRDC, <http://grdc.bafg.de>). Annual average inflow ($0.029 S_v$, $S_v = 10^6 \text{ m}^3 \text{ s}^{-1}$) is used in the standard run (simulations with river inflow) to investigate the influence of Changjiang discharge on regional circulation. The daily outputs of temperature, salinity and velocity (u , v) in the East China Sea (119–126°E,

Table 1. Simulation scenarios.

Swimming schemes	Control runs (a)	Standard runs (b)
Scheme 0: no active swimming	0a	0b
Scheme 1: swimming along with the current	1a	1b
Scheme 2: stepwise change depending on temperature	2a	2b

The numbers represent different swimming schemes of fish: scheme 0, no active swimming; scheme 1, swimming along with the current; scheme 2, stepwise change in orientation depending on temperature (see text for detail). In control runs, the circulation model did not include the Changjiang discharge.

24–33°N) were stored for offline particle tracking simulation to reduce the simulation time. Temporal sensitivity tests on the offline model indicate that, although some minor uncertainty exists, the dominant winter feature of CCC guides most of the particles moving along similar paths consistently (data not shown). Thus, daily outputs are reasonably chosen in a statistical sense.

Biological model: Lagrangian particle tracking simulation

A Lagrangian particle tracking simulation program was used to simulate fish migration. Each tracer in simulation can be viewed as a ‘super-individual’— a small group of anchovies. A total of 50 tracers was released uniformly at 121–125°E, 31°N and assumed to stay at a constant depth (12.5 m) during the simulation. We chose 12.5 m because the previous acoustic survey in the ECS showed that the vertical distribution of Japanese anchovy might be homogeneous and concentrated between 5 and 20 m in winter (Iversen *et al.*, 1993) and 12.5 m is the average depth of the Japanese anchovy stock. We assumed no vertical migration of anchovies because vertical migration is insignificant in winter and early spring according to field observations (Iversen *et al.*, 1993). The initial locations were determined according to field observations (Iversen *et al.*, 1993). Preliminary simulations showed that the tracers released from 125 to 130°E would follow the Kuroshio northward; hence the southward-migrating anchovy stock was not likely to be located near the shelf break of ECS east of 125°E. Because the maximum CPUE of larval anchovy lies in March (Fig. 1b) with an age of 15–30 days (Chiu and Chen, 2001), the spawning stock must start migrating in January and arrive at known spawning grounds (northeastern Taiwan) before the end of February in order to have a successful recruitment. Therefore, all

simulations started on the first day of January (day 1) and terminated on the last day of February (day 59) in the hypothesis testing. The starting date of spawning migration was further investigated by sensitivity analyses.

Biological model: fish swimming behavior

The swimming behavior of adult anchovies is included in the particle tracking model. The behavior can be decomposed into two parts: orientation and velocity. In our swimming behavior model, the orientation of migration can be determined by either current velocity (Eqn 1) and/or temperature gradient (Eqns 2–4):

$$V = 30 \text{ cm/s}$$

$$u_{s1} = V \cdot \frac{u_c}{\sqrt{u_c^2 + v_c^2}}, v_{s1} = V \cdot \frac{v_c}{\sqrt{u_c^2 + v_c^2}} \quad (1)$$

$$\nabla T = \frac{\partial T}{\partial x} \hat{i} + \frac{\partial T}{\partial y} \hat{j} \quad (2)$$

$$GM = \sqrt{(\partial T / \partial x)^2 + (\partial T / \partial y)^2} \quad (3)$$

$$u_{s2} = V \times \frac{(\partial T / \partial x)}{GM} \hat{i}, v_{s2} = V \times \frac{(\partial T / \partial y)}{GM} \hat{j} \quad (4)$$

Here, V is the magnitude of fish swimming velocity, T is the temperature, GM is the magnitude of temperature gradient u_c , v_c represent the x , y component of current velocity at the initial depth of the tracers, and u_{s1} , v_{s1} , u_{s2} and v_{s2} represent the x , y component of fish swimming velocity in the two swimming schemes. The current velocity was derived from the average of the first layer (6 m) and second layer (20 m) from the TIMCOM model, which is largely consistent with the depth of anchovy. Equation (1) describes the fish swimming in alignment with the current (u_{s1} , v_{s1}). Previous research using electric tagging on Pacific salmon suggests that drifting with currents may potentially help the migratory fishes to cover more distance (Tanaka *et al.*, 2005). We assumed that Japanese anchovy might employ the similar strategy by swimming along with the current. As anchovy is a slow swimmer (Masuda, 2011), swimming along with the current would be beneficial for conserving energy during spawning migration.

The swimming behavior modeled by Eqns (2–4) (u_{s2} , v_{s2}) indicates that the fish swim toward the

local region of maximum temperature. This may be physiologically beneficial to anchovies because the growth rate of eggs and larvae is greater in warm conditions. It has been observed that migratory routes of fishes are often affected by ocean fronts such as steep salinity and/or temperature gradients (Leggett, 1977). Swimming against the current is possible if the local maximum of temperature is in a counter-current direction from the perspective of fish.

The assumed swimming velocity is inferred from previous theoretical studies. Usually, fish swimming consists of spontaneous bursts and periodic cruising (Sfakiotakis *et al.*, 1999). During the cruise migration, the cruise speed must be optimized to save energy. The optimal cruise speed of fish for maximum moving range is about one body length (cm s^{-1} ; Weihs, 1973). However, occasional bursts should also be taken into account. We assume that the swimming speed of migrating groups is 30 cm s^{-1} (approximately two body lengths per second) in this swimming behavior model. Initial tests on swimming speed showed that 30 cm s^{-1} is the minimum requirement for the tracers to reach the coastal area of Taiwan within the simulation period. Note that the vertical swimming velocity is ignored in this behavior model because vertical migration behavior of Japanese anchovy is not significant in late winter (Iversen *et al.*, 1993).

Based on the two different orientations defined by the Eqns (2–4), three different swimming schemes are derived:

0 Passive: no active swimming behavior.

1 Swimming along with the current (Eqn 1).

2 Stepwise: swimming along with the current (Eqn 1) and then changing to swimming toward the region of maximum temperature (Eqns 2–4) when the optimal temperature for spawning is sensed.

The 'stepwise' approach is developed as an improvement of Eqns (2–4). Preliminary modeling results showed that when fish persistently swim toward the region of maximum temperature (Eqns 2–4), all fish swim offshore. This is because the sea surface temperature is higher in the offshore area, where the Kuroshio is present, than in the inshore area; hence, all tracers will eventually move toward the offshore area and hardly approach the coastal area of Taiwan. As this result contradicts the existed fishery practices in the coastal area of Mainland China and Taiwan, the modified version 'stepwise' swimming scheme (combined Eqns 1–4) was used to describe the swimming behavior of fish. In the 'stepwise' swimming scheme, the migrating group first swims along with the current, and then swims toward the region of maximum temperature when the optimal temperature for

spawning is sensed in the perceptible distance. The perceptibility of the migrating group is 10 m from the centroid of the group. The temperature field was interpolated into 10-m resolution by a linear method before computing the gradient. The optimal temperature for spawning is set as $22 \text{ }^\circ\text{C}$ based on observations of high spawning frequency of Japanese anchovies (Takasuka *et al.*, 2005) and optimal growth rate for larval anchovies (Takasuka and Aoki, 2006). The swimming schemes were tested in both control (without river discharge) and standard runs (with river discharge). The experimental scenarios are summarized in Table 1.

Sensitivity analyses

The sensitivity analyses of fish behavior–hydrodynamic coupled model consist of three components: optimal spawning temperature, initial locations, and starting dates. As mentioned in Takasuka *et al.* (2005), the optimal spawning temperature of Japanese anchovy shows large geographical variations. Different optimal temperatures, ranging from 20 to $24 \text{ }^\circ\text{C}$, were tested with the same initial setting as in experiment 2b.

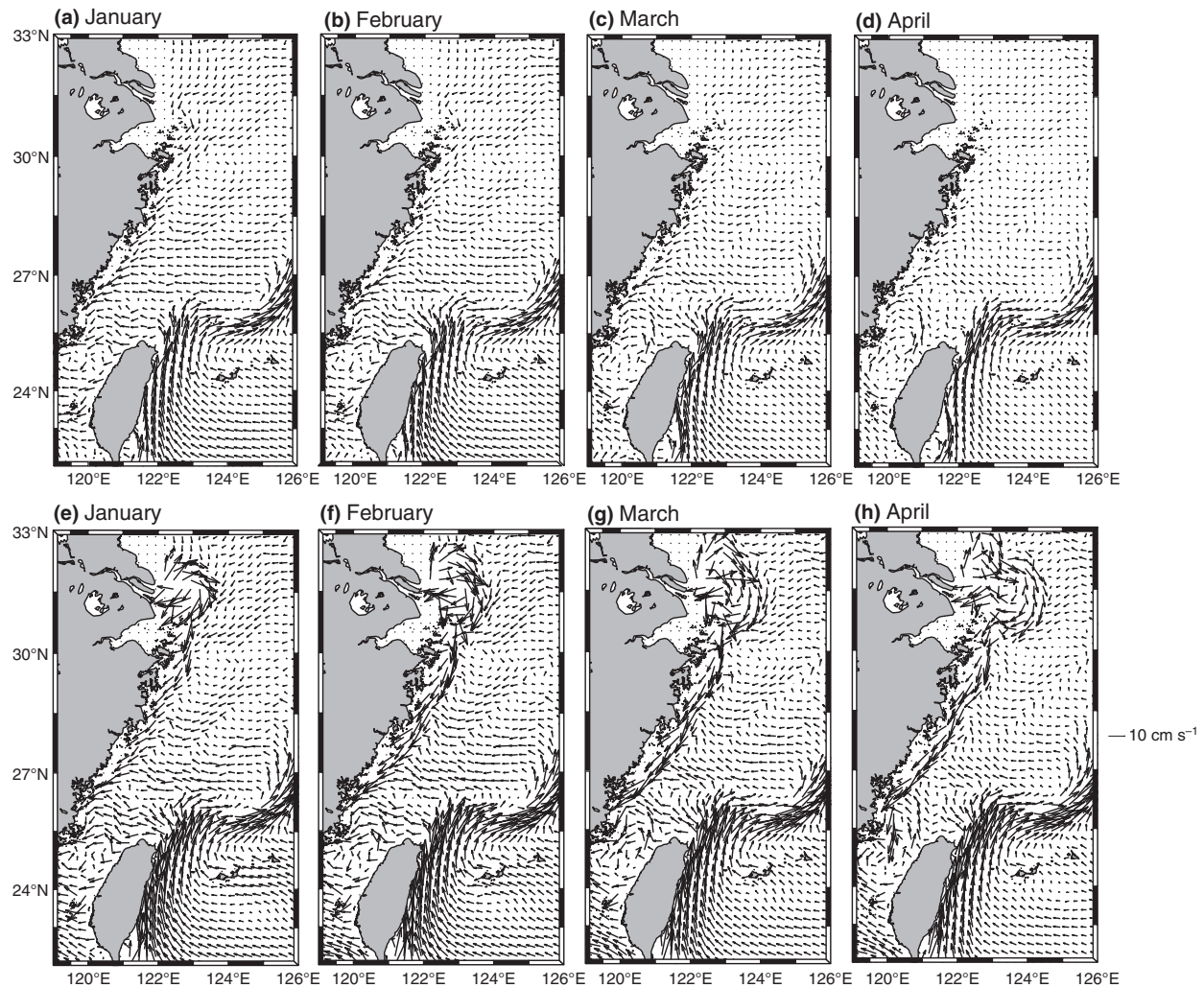
In the sensitivity test of initial locations, two different locations (30 and 32°N) were examined according to the northernmost and southernmost distribution of the overwintering adult anchovy stocks observed in the acoustic surveys (Iversen *et al.*, 1993). The sensitivity test on starting dates keeps the same initial locations (121 – 125°E , 31°N) but releases the Lagrangian tracers every 5 days. A total 13 simulations were performed (spanning approximately 2 months). After simulation, the tracers with final location south of 25.5°N , north of 24.5°N , and between 120.5 and 122.5°E are considered to have 'arrived' at the suitable spawning ground around the coastal region of Taiwan.

RESULTS

The physical environment

Our physical model successfully reproduces the seasonal hydrography of the ECS, including the surface circulation due to the Changjiang discharge (Fig. 3) and hydrographic characteristics (Figures 4 and 5) along the coast of mainland China. The freshwater of Changjiang enters the ECS and forms the Changjiang Diluted Water (CDW) plume (Fig. 3e–h) with lower temperatures and salinity compared with the offshore seawater (Figures 4e–h and 5a–d). The cold, low density freshwater at the surface forms an anticyclonic eddy in the frontal area. Due to a balance between density gradient and Coriolis forces, the CDW forms a southward jetstream along the coast of mainland China, the

Figure 3. Distribution of monthly mean near-surface (first layer of the model output) current velocity in the (a–d) control and (e–h) standard runs. The China Coastal Current becomes noticeable in early spring.



CCC. The CCC forms an ocean front in the sea surface temperature (Fig. 4e–f), commonly observed in satellite images (Chang *et al.*, 2006). In spring, the CCC starts to weaken owing to the developing East Asian summer monsoon (Figures 4g–h and 5c–d). It is worth noting that the simulation results of the monthly mean near-surface current indicate that the CCC is much stronger in the standard run (Fig. 3e–f) than with the control simulation (Fig. 3a–d).

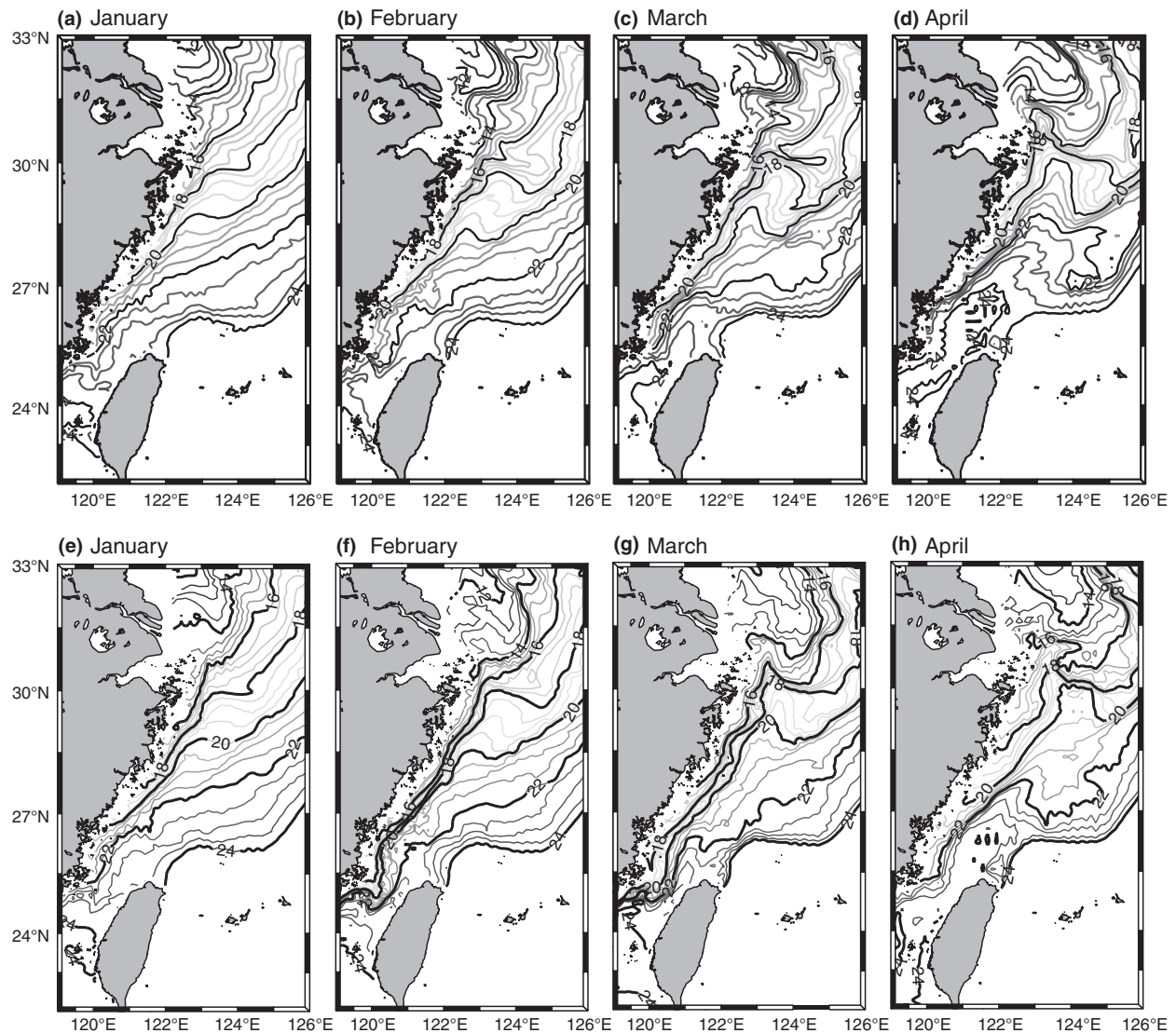
In addition, the Kuroshio passes the east coast of Taiwan and continues to flow north of Ryukyu Island (Fig. 3). The Taiwan Strait throughflow shows clear monthly variations in model runs (Fig. 3). In winter, the northeastern monsoon impedes the northward transport of Taiwan Strait (Fig. 3a–b,e–f), and the northward transport of Taiwan Strait Current is enhanced as the northeastern monsoon wanes in spring

(Fig. 3c–d,g–h). These simulation results generally agree well with observations (Jan *et al.*, 2006). Further validation between model outputs and observations can be found in Jan *et al.* (2010).

Tracer trajectories of the spawning migration simulations

Experiment 0: Passive. The Changjiang discharge significantly affects the tracer trajectories, according to the comparison of the standard and control runs in experiment 0 (Fig. 6a,c; cf. Fig. 2). The major difference lies in the direction of motion of tracers. Almost all tracers follow the orientation of the CCC and move southward in the standard run. By contrast, only a small portion of tracers that started nearshore (122.5–123.3°E) move southward in the control run. Another difference is the final locations of the tracers. The tracers can reach about 25°N (coastal area of

Figure 4. Monthly mean near-surface water temperature in the control (a–d) and standard (e–h) run. When river discharge is present (standard run), the Changjiang dilution water forms a front along the coast of China. The front is less significant in the control run.



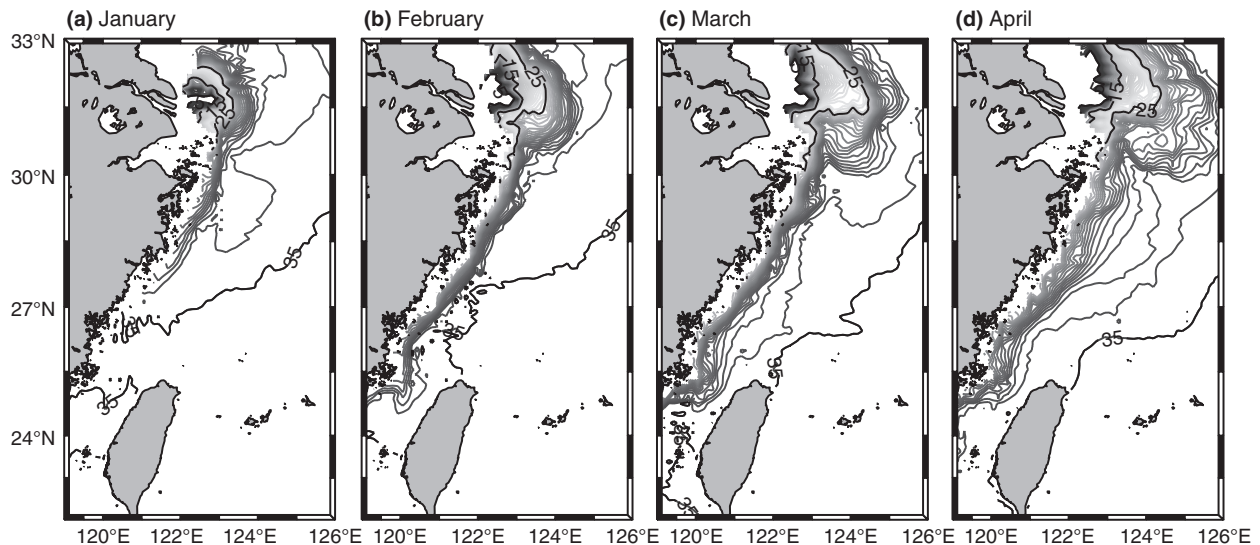
Putian, Fujian Province) in the standard run, whereas tracers can only reach about 26°N (coastal area of Ningde, Fujian Province) in the control run. However, all tracers in both runs fail to cross the Taiwan Strait to approach the coastal area of Taiwan. Based on this experiment, we can conclude that the spawning migration of Japanese anchovy from the ECS to Taiwan is definitely aided by the CCC and is unlikely to be passive.

Experiment 1: Swimming along with current. The tracer simulations including the swimming behavior generally arrive earlier than those without swimming

behavior (Experiment 0). For example, the nearshore tracers (122.5–123.3°E) in Experiment 1 (Fig. 6b,d) reach the same point about 2 weeks earlier than those in Experiment 0 (Fig. 6a,c) because of the extra velocity gained from swimming. In addition, most of tracers remain in the Changjiang River Plume in the control run (Fig. 6b), whereas in the standard run, only tracers starting at 124.25–124.5°E were trapped around the plume region (Fig. 6d).

Even though the tracers in experiment 1 move much faster than those in experiment 0, all tracers cruise around in the middle of the Taiwan Strait and fail to approach the coastal area of Taiwan at the end of sim-

Figure 5. Monthly average near-surface salinity in the standard run (a–d) showing how low-salinity Changjiang Diluted Water intrudes southward and contributes to the China Coastal Current. The salinity in the China Coastal Current is 30–31 psu, much lower than the surrounding areas.



ulations. This is consistent with the observation that the CCC always flows along the coast of China. The results suggest that swimming scheme 1 (swimming along with the current) may only partially represent the actual swimming behavior of Japanese anchovies.

Experiment 2: Stepwise-swimming along current until sensing optimum spawning temperature (22 °C). Experiment 2 with stepwise-swimming scheme is the only simulation in which tracers reach the coastal area of Taiwan within the simulation period. In the control run, the nearshore tracers also move southward but split into two groups and stop in the middle of the Taiwan Strait (Fig. 7a). The tracers in the standard run arrive at the coastal area of Taiwan (Fig. 7b) at the end of the simulation (day 59). The difference in the two simulation runs can be explained by the thermal front along the coast of mainland China (Fig. 4). The frontal temperature gradient is more prominent in the standard run. As the swimming direction of scheme 2 is determined by the temperature gradient within a 10-m grid, the larger temperature gradient can result in a stronger directional movement in the standard run.

The results in Experiment 2 suggest that the ‘stepwise’ swimming scheme is more likely to represent the behavior of Japanese anchovy migrating from the ECS to the coastal waters of Taiwan. This scheme includes a biological swimming behavior. It is also worth noting that stepwise-swimming scheme simulation produces more than one migration route to the known fishing grounds (Fig. 7b).

Sensitivity analyses

The sensitivity analysis on initial locations indicates that the tracer trajectories in the experiment 2 (Fig. 7c,d) are quite representative. In this simulation, the north and south boundary of the anchovy overwintering ground is used as the initial locations. Although the trajectories may vary, most of the tracers reach the coastal area of Taiwan (Fig. 7c,d). Therefore, the migration route of Japanese anchovies is likely to follow the CCC regardless of the initial locations of 30 or 32°N.

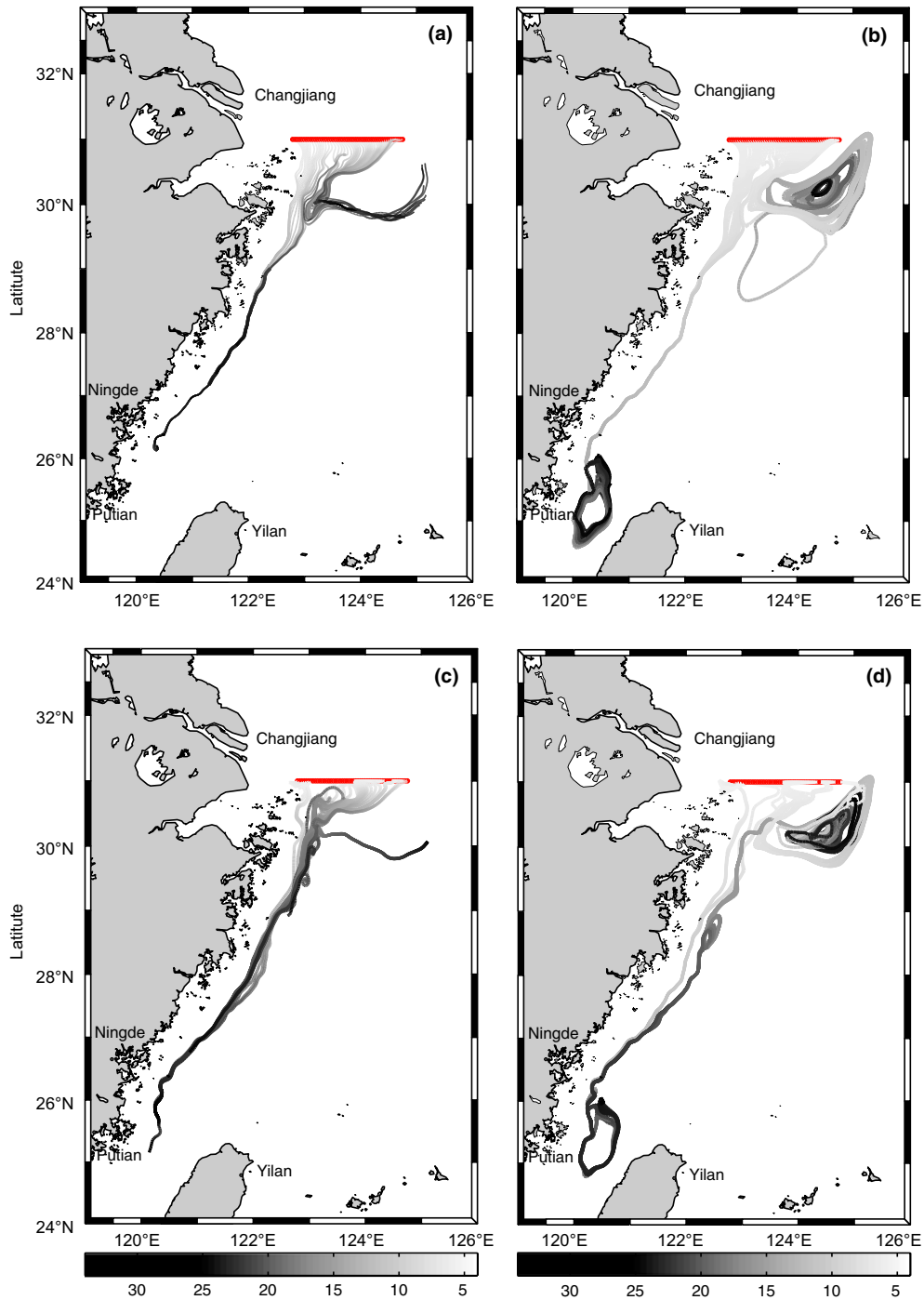
The sensitivity test of the particle-released starting dates shows that the number of tracers reaching the coastal waters of Taiwan decreases with the delayed starting dates (Fig. 8). With a 25-day delay, the number of arrived tracers does not vary substantially. The arrivals decrease about 20% if the starting date is later than 25 January. Therefore, the onset of migration is most likely to start in January and is closely related to the strength of CCC. In addition to starting dates, the number of arrived tracers also appears to be sensitive to the optimal spawning temperature (Fig. 9). Nevertheless, the setting of 22 °C produces the best results (highest number of tracers arrived).

DISCUSSION

Model evaluation – comparing simulation results with fisheries records

The simulation results confirm the previous speculation that the CCC is critical for the spawning

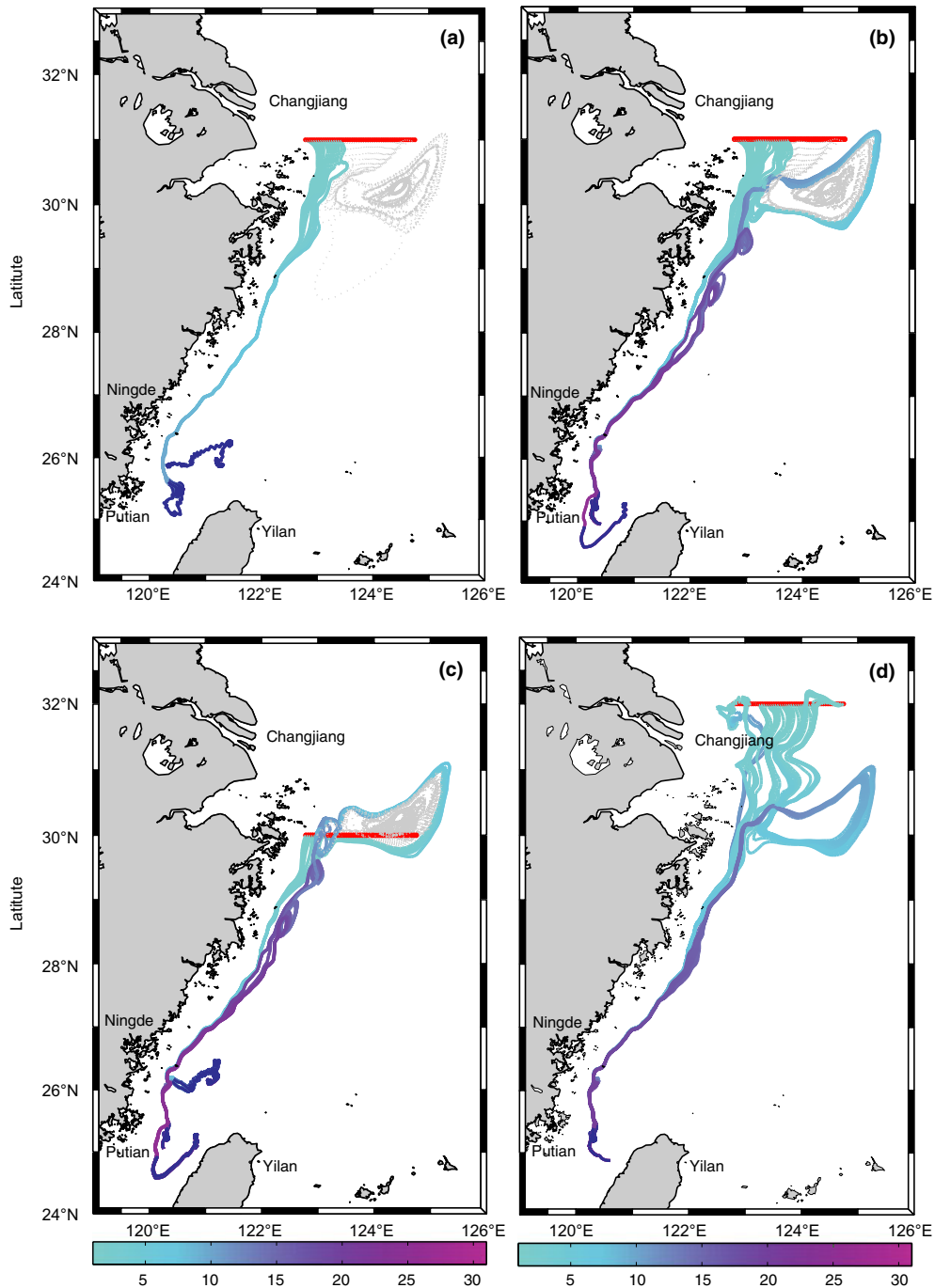
Figure 6. Tracer trajectories of numerical experiments with Changjiang discharge-excluded control runs (a,b) and discharge-included standard runs (c,d). None of the tracers reached the coastal area of Taiwan with swimming scheme 1 (b,d) or without swimming (a,c). The initial locations of the tracers are collectively shown as a red bar. The tracer trajectories are represented by grayscale lines, which also denote the simulation days.



migration of Japanese anchovy (Figures 6 and 7). The tracer trajectories also show a good agreement with existing fishing grounds of Japanese anchovy larvae in the coastal waters of Taiwan and mainland China. For

example, according to a previous report (Chen *et al.*, 2010), two fishing grounds for larval Japanese anchovy exist in Northern Taiwan: the western fishing ground in the eastern Taiwan Strait (with a relatively smaller

Figure 7. Tracer trajectories of stepwise swimming schemes in both runs [(a) control, (b) standard] and the sensitivity analyses on different initial locations (collectively shown as a red bar in the figure): (c) 30°N and (d) 32°N. The color scale from cyan to magenta represents the simulation days from 1 to 31; the blue line denotes the period when tracers move toward optimal spawning temperature. The gray dotted lines represent the tracers remained at the ECS. Only tracers of stepwise swimming scheme in standard run eventually reached the coastal area of Taiwan (b). The sensitivity analysis on two different initial locations using the experiment 2b setting (see Table 1) shows the robustness of stepwise swimming scheme (c,d).



catch) and the eastern fishing ground in the north-western Pacific Ocean (Yilan Bay, the main larval anchovy fishing ground). In experiment 2b (standard

run, Fig. 7b) and sensitivity test of initial locations (Fig. 6c,d), many tracers reach the fishing ground in the eastern Taiwan Strait at the end of February (blue

Figure 8. Summary statistics of simulations with delayed initial day. The bottom dates correspond to the calendar dates of initial particle release. The total number of arrived tracers decreases about 20% when the onset of simulation is later than January (Day 30). No tracer reached the coastal area of Taiwan after February.

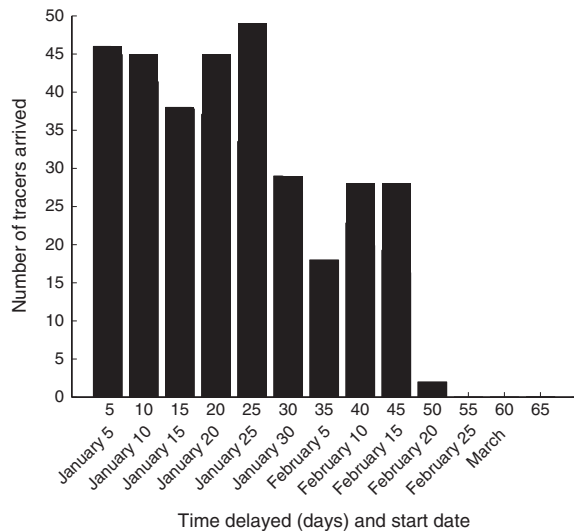
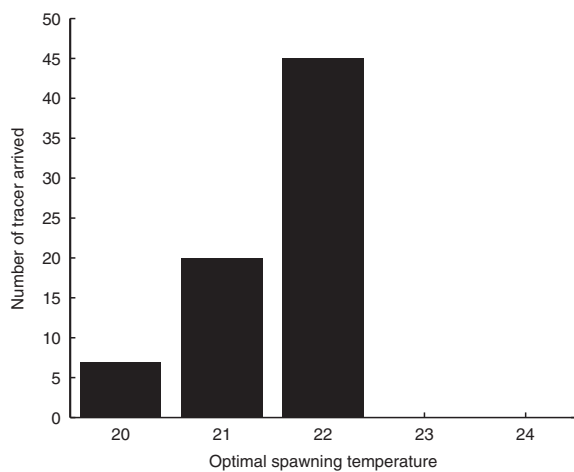


Figure 9. Summary statistics of sensitivity analysis with different optimum spawning temperature setting from 20 to 24 °C.



line in Fig. 7), although no tracers reach Yilan Bay. In addition, the simulated migration route and timing also matches the adult anchovy fishery in the southeastern coast of mainland China. The fishing season of Japanese anchovies in Fujian Province generally starts in February, targeting the adult overwinter group first, and then the larvae and juveniles in the spring (Fujian Fauna and Flora Editing Committee, 2003).

Our model results demonstrate the advantage of the Lagrangian model in testing possible migration routes and behavior scenarios. The spawning stock of Japanese anchovy is most likely to follow the CCC and move from the ECS to the coastal waters of Taiwan. However, no tracer reaches Yilan Bay, suggesting that either the biological or the physical model needs further improvements. Indeed, empirical observations show a nearshore coastal current in northern Taiwan (Tang *et al.*, 2000), which may facilitate the migration of the spawning stock of anchovies from the Taiwan Strait (west) to the Yilan Bay (east). However, such a current was not present in our physical model simulation (Fig. 3e–h). Most basin-scale ocean circulation models cannot capture such coastal processes in detail due to the lack of required model resolution.

Fluctuation of Japanese anchovy and the potential impacts of Changjiang discharge variation in the East China Sea

As an important fisheries resource, the fluctuation of Japanese anchovy has caught the attention of fisheries scientists for decades (Hayashi, 1966). It was suggested that the synchronous variation of the catch in the Pacific over 50 yrs reflects the basin-scale regime shift of climate (Chavez *et al.*, 2003). The ‘optimal temperature hypothesis’ further suggests that higher temperature favors faster growth of larval anchovies and that this climate shift is the main driving force behind the fluctuations of anchovy in the Northwestern Pacific (Takasuka *et al.*, 2007). However, this scenario may not be the only explanation for all Japanese anchovy stock variations. The analysis of the larval anchovy CPUE southwest off Taiwan (Hsieh *et al.*, 2009), for example, has shown that the dynamics of the anchovy population may be affected not only by basin-scale hydrographic conditions; other factors, such as strength of the CCC, might also affect the anchovy group migrating toward coastal waters of Taiwan. Our modeling results indeed highlight the importance of the CCC in affecting spawning migration of Japanese anchovy.

In addition, our simulations focusing on the spawning stock of Japanese anchovy in northeastern Taiwan demonstrate that the change of Changjiang discharge may have potential impacts on the recruitment of Japanese anchovy. The weakened CCC caused by reduced river discharge of Changjiang could decrease the flux of anchovy population arriving on the coast of Taiwan, which may further affect the recruitment process; we speculate that this will eventually cause a decline in the stock. The Changjiang discharge has indeed revealed a decreasing trend in the past four decades, possibly due to increased water

consumption and reservoir construction (Yang *et al.*, 2005). As TGD was established in 2005, the intensified human activities in the Changjiang catchment may continue to influence the river discharge and thus the CCC.

In addition to the direct effect of weakening CCC, TGD may also threaten the anchovy stocks by inducing ecosystem changes in the ECS. Damming can alter the chemical loads of the river (Mitkees *et al.*, 1972) and consequently change the biogeochemistry and planktonic communities (Nixon, 2003). Field measurements of primary production suggest that the ECS ecosystem is sensitive to the change in water outflow, and the primary production has declined 86% from 1998 to 2003 (Gong *et al.*, 2006). This decline in primary production may have a bottom-up effect on the spawning stocks of Japanese anchovy, as the adult anchovies forage in the ECS. The example of the Aswan High Dam in Egypt has shown that once the dam was constructed, the phytoplankton blooms associated with Nile floods disappeared. As a consequence, the catches of sardines in the Egyptian Mediterranean off the Nile decreased from 15 000 to 554 t from 1964 to 1966 (Aleem, 1972). However, the fishery landings have rebounded dramatically since the 1980s, which may suggest that human sewage and agricultural drainage are replacing the role of Nile as an inorganic nutrient supply (Nixon, 2003). Nonetheless, we should not be too optimistic about the recovery of the anchovy population in the ECS and its adjacent fishing grounds. Recent studies have shown that fishing can enhance the sensitivity of the population toward environmental changes (Hsieh *et al.*, 2006, 2008). While the fishing pressure and other unfavorable environmental conditions such as hypoxia (Chen *et al.*, 2007) are still present, how the Japanese anchovy population will respond to those changes remains to be answered.

Implications for fisheries ecology

Coupled biological–physical modeling is playing an increasingly important role in ecosystem-based approach to fisheries (de Young *et al.*, 2004; Plagányi 2007; Townsend *et al.*, 2008). For migratory fishes, spatial components have been included in models such as Atlantis, GADGET, and Ecopath with Ecosim coupled with Ecospace (Plagányi 2007). However, these systems do not model the swimming behavior of fish explicitly; instead, they use probabilistic allocation functions to re-distribute stocks. Fully coupled ecosystem–fish behavior models, such as NEMURO.FISH (Ito *et al.*, 2004) and SEAPODYM (Bertignac *et al.*, 1998; Lehodey *et al.*, 1998, 2008), have also been developed. NEMURO.FISH is an individual-based

model specified with the bioenergetics of fish, but the migration of fish is prescribed rather than the behavioral response to the environment. SEAPODYM, by contrast, is a Eulerian approach model using advection–diffusion reaction formulation to describe the spatial dynamics of fish populations (Bertignac *et al.*, 1998; Lehodey *et al.*, 1998, 2008). In SEAPODYM, the movement of fishes is determined by the habitat preference (e.g., temperature, food) in the environment. Our model is an individual-based Lagrangian simulation, and the decision of fish movement is similar to the approach of SEAPODYM. But the Lagrangian modeling approach does not require detailed information on the spatial distribution of fish. Hence, we can simulate the migration of a stock from various locations and explore possible starting points when such data are unavailable.

Although our experiment shows that the biological model may catch the essential of Japanese anchovy migration behavior, such a primitive model tends to oversimplify fish biology. Previous research on spawning migration modeling in capelin and cod (Huse *et al.*, 2004) and Japanese sardine (Okunishi *et al.*, 2009) has demonstrated other possible approaches to simulating the swimming behavior of migratory fish. The model study of capelin and cod in the Barents Sea (Huse *et al.*, 2004) combines an individual-based swimming behavior model with observed temperature distribution. The results show that the model can partially reproduce the spatial dynamics of both species. However, the swimming direction is predetermined rather than estimated based on environmental cues. By contrast, Okunishi *et al.* (2009) combined the bioenergetics model (NEMURO.FISH by Ito *et al.*, 2004), a genetic algorithm (GA), and an artificial neural network (ANN) to simulate the migration of Japanese sardine in the western North Pacific. The swimming direction was determined by environmental factors, such as temperature experienced by fishes and the length of day, through empirical training by ANN. Such an empirical modeling approach based on ANN requires field observation data for the training process, and thus the simulation of the realistic spawning migration using GA and ANN can be constrained by the availability of data.

One important caveat of our model is that we do not include ecosystem components (lower trophic levels) or bioenergetics of fish. The coupled physical circulation model with lower-trophic level foodweb model and fish bioenergetics model (e.g., NEMURO.FISH) has been used to reproduce the growth and many biological processes of European anchovy in Mediterranean (Politikos *et al.*, 2011). Besides

temperature, foraging is one of the important factors in fish migration (Leggett, 1977). The prey field is known to be crucial in determining the spawning location, as shown in European anchovy in the Mediterranean (Palomera, 1992). Whereas the hydrographic features help the retention of anchovy egg and larvae (Cuttitta *et al.*, 2003), the high prey density and suitable temperature can maximize the larval growth and increase their survival rate. Therefore, future developments including ecosystem and bioenergetics components will be useful for a better understanding of the spatial-temporal dynamics of Japanese anchovy. Nevertheless, although simplified, our model is still useful for scenario exploration and may provide guidance in studying anchovy migration and information for fisheries management.

CONCLUSION

We demonstrated the usefulness of a coupled fish behavior-hydrodynamic model to achieve a better understanding of the influence of different environmental and behavioral scenarios on Japanese anchovies. Our simulation shows that spawning migration of Japanese anchovy is likely to be aided by regional circulation, importantly the CCC. Moreover, the swimming behavior of fish can also play an important role during their migration. The TGD was completed in 2005, and the reduced Changjiang discharge and nutrient input may continue to affect the Japanese anchovy population. More ecological studies using fishery-independent data, such as behavior, spatial distribution, and life history characteristics, are necessary for a better understanding of the fluctuation of Japanese anchovy population in the ECS.

ACKNOWLEDGEMENTS

Discussion with Takeshi Miki and Sen Jan greatly improved this work. We are grateful for the comments from Chih-Shin Chen, Wen-Bin Huang and Shin-ichi Ito. This research is supported by a grant for Frontier and Innovative Research of National Taiwan University and National Science Council, Taiwan.

REFERENCES

- Aleem, A.A. (1972) Effect of river outflow management on marine life. *Mar. Biol.* **15**:200–208.
- Bertignac, M., Lehodey, P. and Hampton, J. (1998) A spatial population dynamics simulation model of tropical tunas using a habitat index based on environmental parameters. *Fish. Oceanogr.* **7**:326–334.
- Capella, J.E., Quetin, L.B., Hofmann, E.E. and Ross, R.M. (1992) Models of the early life history of *Euphausia superba* – Part II. Lagrangian calculations. *Deep-Sea Res.* **39**:1201–1220.
- Chang, Y., Shimada, T., Lee, M.A., Lu, H.J., Sakaida, F. and Kawamura, H. (2006) Wintertime sea surface temperature fronts in the Taiwan Strait. *Geophys. Res. Lett.* **33**:L23603.
- Chavez, F.P., Ryan, J., Lluch-Cota, S.E. and Niquen, C.M. (2003) From anchovies to sardines and back: multidecadal change in the Pacific Ocean. *Science* **299**:217–221.
- Chen, C.S. and Chiu, T.S. (2003) Early life history traits of Japanese anchovy in the northeastern waters of Taiwan, with reference to larval transport. *Zool. Stud.* **42**:248–257.
- Chen, C., Gong, G. and Shiah, F. (2007) Hypoxia in the East China Sea: one of the largest coastal low-oxygen areas in the world. *Mar. Environ. Res.* **64**:399–408.
- Chen, C.S., Tzeng, C.H. and Chiu, T.S. (2010) Morphological and molecular analyses reveal separations among spatio-temporal populations of anchovy (*Engraulis japonicus*) in the southern East China Sea. *Zool. Stud.* **49**:270–282.
- Chiu, T.S. and Chen, C.S. (2001) Growth and temporal variation of two Japanese anchovy cohorts during their recruitment to the East China Sea. *Fish. Res.* **53**:1–15.
- Chiu, T.S., Young, T.S. and Chen, C.S. (1997) Monthly variation of larval anchovy fishery in I-lan bay, NE Taiwan, with an evaluation for optimal fishing season. *J. Fish. Soc. Taiwan* **24**:273–282.
- Cowen, R.K., Paris, C.B. and Srinivasan, A. (2006) Scaling of connectivity in marine populations. *Science* **311**:522–527.
- Cushing, D.H. (1975) *Marine Ecology and Fisheries*. Cambridge: Cambridge University Press, 278 pp.
- Cuttitta, A., Carini, V., Patti, B. *et al.* (2003) Anchovy egg and larval distribution in relation to biological and physical oceanography in the Strait of Sicily. *Hydrobiologia* **503**:117–120.
- Dietrich, D.E., Mehra, A., Haney, R. *et al.* (2004) Dissipation effects in North Atlantic Ocean modeling. *Geophys. Res. Lett.* **31**:L05302.
- Dietrich, D.E., Tseng, Y.H., Medina, R. *et al.* (2008) Mediterranean Overflow Water (MOW) simulation using a coupled multiple-grid Mediterranean Sea/North Atlantic Ocean model. *J. Geophys. Res.* **113**:C07027.
- Fujian Fauna and Flora Editing Committee (2003) *Chorography of Fujian Province Volume 10: Fauna and Flora of Fujian Province [in Chinese]*. Beijing: Fangzhi Press, 541–542 pp.
- Gong, G.C., Chang, J., Chiang, K.P. *et al.* (2006) Reduction of primary production and changing of nutrient ratio in the East China Sea: effect of the Three Gorges Dam. *Geophys. Res. Lett.* **33**:1–4.
- Hayashi, S. (1966) A note on the biology and fishery of the Japanese anchovy *Engraulis japonica* (Houttuyn). *CalCOFI Rep.* **11**:44–57.
- Hellerman, S. and Rosenstein, M. (1983) Normal monthly wind stress over the world ocean with error estimates. *J. Phys. Oceanogr.* **13**:1093–1104.
- Hsieh, C.H., Reiss, C.S., Hunter, J.R., Beddington, J.R., May, R.M. and Sugihara, G. (2006) Fishing elevates variability in the abundance of exploited species. *Nature* **443**:859–862.
- Hsieh, C.H., Reiss, S.C., Hewitt, R.P. and Sugihara, G. (2008) Spatial analysis shows fishing enhances the climatic sensitivity of marine fishes. *Can. J. Fish. Aquat. Sci.* **65**:947–961.

- Hsieh, C.H., Chen, C.S., Chiu, T.S. *et al.* (2009) Time series analyses reveal transient relationships between abundance of larval anchovy and environmental variables in the coastal waters southwest of Taiwan. *Fish. Oceanogr.* **18**:102–117.
- Huse, G., Johansen, G.O., Bogstad, B. and Gjøsaeter, H. (2004) Studying spatial and trophic interactions between capelin and cod using individual-based modeling. *J. Mar. Sci.* **61**:1201–1213.
- Ito, S.I., Kishi, M.J., Kurita, Y. *et al.* (2004) Initial design for a fish bioenergetics model of Pacific saury coupled to a lower trophic ecosystem model. *Fish. Oceanogr.* **13**:111–124.
- Iversen, S.A., Zhu, D., Johannessen, A. and Toresen, R. (1993) Stock size, distribution and biology of anchovy in the Yellow Sea and East China Sea. *Fish. Res.* **16**:147–163.
- Jan, S., Sheu, D.D. and Kuo, H.M. (2006) Water mass and throughflow transport variability in the Taiwan Strait. *J. Geophys. Res.* **111**:1–15.
- Jan, S., Tseng, Y.H. and Dietrich, D. (2010) Sources of water in the Taiwan Strait. *J. Oceanogr.* **66**:211–221.
- Lee, C., Liu, D.C. and Su, W.C. (2009) Seasonal and spatial variations in the planktonic copepod community of Ilan Bay and adjacent Kuroshio waters off northeastern Taiwan. *Zool. Stud.* **48**:151–161.
- Leggett, W.C. (1977) The ecology of fish migrations. *Ann. Rev. Ecol. Syst.* **8**:285–308.
- Lehodey, P., Andre, J., Bertignac, M. *et al.* (1998) Predicting skipjack tuna forage distributions in the equatorial Pacific using a coupled dynamical bio-geochemical model. *Fish. Oceanogr.* **7**:317–325.
- Lehodey, P., Senina, I. and Murtugudde, R. (2008) A spatial ecosystem and populations dynamics model (SEAPODYM) – Modeling of tuna and tuna-like populations. *Prog. Oceanogr.* **78**:304–318.
- Levitus, S. and Boyer, T.P. (1994) *World Ocean Atlas 1994, Vol. 4: Temperature*. Washington, DC: National Environmental Satellite, Data, and Information Service. PB-95-270112/XAB.
- Ljung, L. (1999) *System Identification: Theory for the User*, 2nd edn. Upper Saddle River, NJ: Prentice Hall.
- Masuda, R. (2011) Ontogeny of swimming speed, schooling behaviour and jellyfish avoidance by Japanese anchovy *Engraulis japonicus*. *J. Fish Biol.* **78**:1323–1335.
- Miller, T.J. (2007) Contribution of individual-based coupled physical–biological models to understanding recruitment in marine fish populations. *Mar. Ecol. Prog. Ser.* **347**:127–138.
- Mitkees, A.I., Zikri, B.S., El-Banna, M.M. and Abou-Zeid, W.A. (1972) Effect of long term storage of the Nile water on its contents of soluble salts and suspended matter. *Agric. Res. Rev.* **50**:31–41.
- Nixon, S.W. (2003) Replacing the Nile: are anthropogenic nutrients providing the fertility once brought to the Mediterranean by a great river? *Ambio* **32**:30–39.
- Okunishi, T., Yamanaka, Y. and Ito, S. (2009) A simulation model for Japanese sardine (*Sardinops melanostictus*) migrations in the western North Pacific. *Ecol. Model.* **220**:462–479.
- Palomera, I. (1992) Spawning of anchovy *Engraulis encrasicolus* in the Northwestern Mediterranean relative to hydrographic features in the region. *Mar. Ecol. Prog. Ser.* **79**:215–223.
- Plagányi, E.E. (2007) Models for an ecosystem approach to fisheries. *FAO Fisheries Technical Paper (FAO)*. No. **477**: 10–20.
- Politikos, D.V., Triantafyllou, G., Petihakis, G. *et al.* (2011) Application of a bioenergetics growth model for European anchovy (*Engraulis encrasicolus*) linked with a lower trophic level ecosystem model. *Hydrobiologia* **670**:141–163.
- Rose, G.A. (1993) Cod spawning on a migration highway in the north-west Atlantic. *Nature* **366**:458–461.
- Sfakiotakis, M., Lane, D.M. and Davies, J.B.C. (1999) Review of fish swimming modes for aquatic locomotion. *IEEE J. Ocean. Eng.* **24**:237–252.
- Shen, M.-L., Tseng, Y.H. and Jan, S. (2011) The formation and dynamics of the cold-dome off northeastern Taiwan. *J. Mar. Syst.* **86**:10–27.
- Sinclair, M. (1988) *Marine Populations: An Essay on Population Regulation and Speciation*. Seattle: Washington Sea Grant Program, 1–252 pp.
- Takasuka, A. and Aoki, I. (2006) Environmental determinants of growth rates for larval Japanese anchovy *Engraulis japonicus* in different waters. *Fish. Oceanogr.* **15**:139–149.
- Takasuka, A., Oozeki, Y., Kubota, H., Tsuruta, Y. and Funamoto, T. (2005) Temperature impacts on reproductive parameters for Japanese anchovy: comparison between in-shore and offshore waters. *Fish. Res.* **76**:475–482.
- Takasuka, A., Oozeki, Y. and Aoki, I. (2007) Optimal growth temperature hypothesis: why do anchovy flourish and sardine collapse or vice versa under the same ocean regime? *Can. J. Fish. Aquat. Sci.* **64**:768–776.
- Tanaka, H., Naito, Y., Davis, N.D., Urawa, S., Ueda, H. and Fukuwaka, M. (2005) First record of the at-sea swimming speed of a Pacific salmon during its oceanic migration. *Mar. Ecol. Prog. Ser.* **291**:307–312.
- Tang, T.Y., Tai, J.H. and Yang, Y.J. (2000) The flow pattern north of Taiwan and the migration of the Kuroshio. *Cont. Shelf Res.* **20**:349–371.
- Townsend, H.M., Link, J.S., Osgood, K.E. *et al.* (eds). (2008) *National Marine Fisheries Service Report of the National Ecosystem Modeling Workshop (NEMoW)*. U.S. Dept. Commerce, NOAA Tech. Memo. NMFS-F/SPO-87, 93 pp.
- Tseng, Y.H., Jan, S., Dietrich, D.E., Lin, I.-I., Chang, Y.T. and Tang, T.Y. (2010) Modeled oceanic response and sea surface cooling to typhoon Kai-Tak. *Terr. Atmos. Oceanic Sci.* **21**:85–98.
- Tseng, Y.H., Shen, M.-L., Jan, S., Dietrich, D.E. and Chiang, C.P. (in press) Validation of the Kuroshio current system in the dual-domain Pacific ocean model framework. *Prog. Oceanogr.*, in press.
- Weih, D. (1973) Optimal fish cruising speed. *Nature* **245**:48–50.
- Yang, S.L., Gao, A., Hotz, H.M., Zhu, J., Dai, S.B. and Li, M. (2005) Trends in annual discharge from the Yangtze River to the sea (1865–2004). *Hydro. Sci. J.* **50**:825–836.
- de Young, B., Heath, M., Werner, F., Chai, F., Megrey, B. and Monfray, P. (2004) Challenges of modeling ocean basin ecosystems. *Science* **304**:1463–1466.
- Yu, H.T., Lee, Y.J., Huang, S.W. and Chiu, T.S. (2002) Genetic analysis of the populations of Japanese anchovy (*Engraulidae: Engraulis japonicus*) using microsatellite DNA. *Mar. Biotech.* **4**:471–479.
- Yu, Z., Kong, X., Chen, C.S., Jiang, Y., Zhuang, Z. and Jin, X. (2005) Mitochondrial DNA sequence variation of Japanese anchovy *Engraulis japonicus* from the Yellow Sea and East China Sea. *Fish. Sci.* **71**:299–307.